

Kinetics and Mechanisms of the Redox Reactions of the Hydroperoxochromium(III) Ion

Wei-Dong Wang, Andreja Bakac,* and James H. Espenson*

Department of Chemistry and Ames Laboratory, Iowa State University, Ames, Iowa 50011

Received June 4, 1993*

The reactions of the hydroperoxochromium(III) ion, $(\text{H}_2\text{O})_5\text{CrO}_2\text{H}^{2+}$ ($\text{CrO}_2\text{H}^{2+}$), with Fe^{2+} , VO^{2+} , V^{2+} , Cu^+ , Ti^{3+} , $\text{Co}(\text{[14]aneN}_4\text{)}^{2+}$, $\text{Co}(\text{Me}_6\text{[14]aneN}_4\text{)}^{2+}$, $\text{Co}(\text{tim})^{2+}$, and $[\text{Ru}(\text{NH}_3)_6]^{2+}$ have been studied in acidic aqueous solution. The reactions are accompanied by large negative entropies of activation, $-110 \text{ J mol}^{-1} \text{ K}^{-1}$ for Fe^{2+} and $-85 \text{ J mol}^{-1} \text{ K}^{-1}$ for Ti^{3+} . All the reactions studied follow an isokinetic relationship in that ΔH^\ddagger is a linear function of ΔS^\ddagger . The same is true for the analogous reactions of H_2O_2 . It is proposed that the reactions of $\text{CrO}_2\text{H}^{2+}$ take place by an inner-sphere, Fenton-type process yielding pentaquaooxochromium(IV), $(\text{H}_2\text{O})_5\text{CrO}^{2+}$ (CrO^{2+}), as an intermediate. The reactivity of $\text{CrO}_2\text{H}^{2+}$ as an oxygen transfer reagent is about 20 times greater than that of H_2O_2 . For example, the reactions with $(\text{en})_2\text{CoSCH}_2\text{CH}_2\text{NH}_2^{2+}$ to yield $(\text{en})_2\text{CoS}(\text{O})\text{CH}_2\text{CH}_2\text{NH}_2^{2+}$ have rate constants $20.5 \pm 0.4 \text{ M}^{-1} \text{ s}^{-1}$ ($\text{CrO}_2\text{H}^{2+}$) and $1.36 \text{ M}^{-1} \text{ s}^{-1}$ (H_2O_2), both in 0.1 M HClO_4 at 25°C . The chromyl ion, CrO^{2+} , oxidizes $\text{CrO}_2\text{H}^{2+}$ to CrO_2^{2+} with a rate constant of $(1.34 \pm 0.06) \times 10^3 \text{ M}^{-1} \text{ s}^{-1}$ in 0.10 M HClO_4 in H_2O and $266 \pm 10 \text{ M}^{-1} \text{ s}^{-1}$ in D_2O .

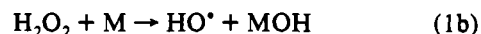
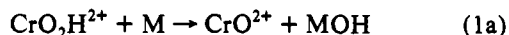
Introduction

The activation of molecular oxygen by aquachromium(II) ion, Cr^{2+} , yields several chromium-containing species, corresponding to different reduction stages of molecular oxygen.¹ One of these species is the hydroperoxochromium(III) ion,^{1b,c} $(\text{H}_2\text{O})_5\text{CrO}_2\text{H}^{2+}$ (henceforth $\text{CrO}_2\text{H}^{2+}$), an analogue of H_2O_2 . Although metal hydroperoxides have been proposed as intermediates in many metal-catalyzed oxidation reactions of organic substrates by H_2O_2 , very little is known about their reactivity.² To compare the redox properties of hydrogen peroxide^{2,3} with that of a metal hydroperoxide, we have studied the reduction of $\text{CrO}_2\text{H}^{2+}$ by ferrous ion.⁴ The reaction takes place by inner-sphere electron transfer and yields a chromyl intermediate. We have now extended our study to a number of transition metal complexes in order to establish the role of the reduction potentials and substitutional lability on the rates of electron transfer.

In the absence of data on similar systems it is impossible to predict the effect of the Cr(III) center on the reactivity of the peroxide. $\text{CrO}_2\text{H}^{2+}$ can formally be regarded as a result of the substitution of one Lewis acid (a proton) in H_2O_2 by another (Cr^{3+}). This might lead one to expect a higher reactivity for $\text{CrO}_2\text{H}^{2+}$ owing to the inductive effect of the trivalent metal center. However, the electronegativity of H^+ is in fact greater than that of Cr^{3+} ,⁵ which would imply that H_2O_2 is a better oxidant than $\text{CrO}_2\text{H}^{2+}$. Admittedly, one has to exercise caution

in using the gas-phase parameters, such as electronegativity, to predict the solution behavior of chemical species. Probably the best solution parameter to consider in the present case is the $\text{p}K_a$ value of the species of interest. The $\text{p}K_a$ for $\text{CrO}_2\text{H}^{2+}/\text{CrO}_2^{2+}$ is unfortunately not known, but if we assume that the effect of Cr(III) will be qualitatively the same at a higher level of protonation, then the values for H_3O_2^+ ($\text{p}K_a -1.7$)⁶ and $\text{Cr}(\text{H}_2\text{O}_2)^{3+}$ ($\text{p}K_a 1-3$)^{1c} provide a good reference point. The much larger $\text{p}K_a$ of $\text{Cr}(\text{H}_2\text{O}_2)^{3+}$ shows that Cr^{3+} has a smaller inductive effect than H^+ and leads to the same conclusion as the gas-phase data, i.e. that H_2O_2 should be a stronger oxidant than $\text{CrO}_2\text{H}^{2+}$.

Any reaction of $\text{CrO}_2\text{H}^{2+}$ by a Fenton-type mechanism would lead to the formation of CrO^{2+} , the Cr(III) analogue of the HO radical, eq 1, as shown previously for the reaction with Fe^{2+} .⁴



The present study of the reduction of $\text{CrO}_2\text{H}^{2+}$ by transition metal reductants was undertaken to find out how general is the formation of CrO^{2+} and whether an inner-sphere path is necessary for the electron transfer to take place. We also studied the reaction of $\text{CrO}_2\text{H}^{2+}$ by CrO^{2+} , whereby $\text{CrO}_2\text{H}^{2+}$ is oxidized to CrO_2^{2+} .

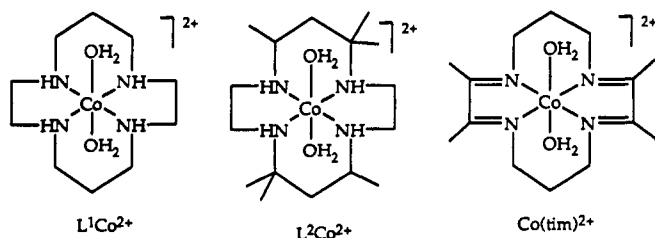
Experimental Section

Reagents. Stock solutions of VO^{2+} were prepared by ion exchanging vanadyl sulfate on a column of Dowex 50W-X4 cation exchange resin. The complex was eluted with 1.93 M HClO_4 . The concentration of VO^{2+} was determined spectrophotometrically ($\epsilon_{660 \text{ nm}} = 17.5 \text{ M}^{-1} \text{ cm}^{-1}$).⁷ Solutions of V^{2+} were prepared by the anaerobic reduction of VO^{2+} over zinc amalgam. The solution of TiCl_3 ^{8,9} in 1.5 M HCl was standardized spectrophotometrically ($\epsilon_{500 \text{ nm}} = 3.9 \text{ M}^{-1} \text{ cm}^{-1}$). The solution of Cu^+ was prepared by Cr^{2+} reduction of Cu^{2+} .¹⁰ The complexes $\text{Co}(\text{[14]aneN}_4)(\text{H}_2\text{O})_2^{2+}$ (L^1Co^{2+}) and $\text{Co}(\text{Me}_6\text{[14]aneN}_4)(\text{H}_2\text{O})_2^{2+}$ (L^2Co^{2+})

* Abstract published in *Advance ACS Abstracts*, October 1, 1993.

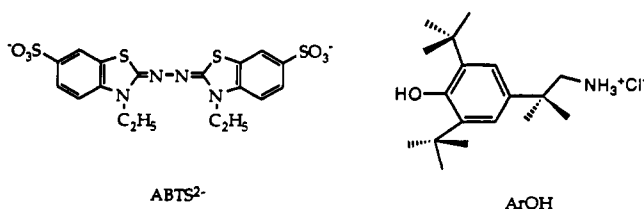
- (1) (a) Brynildson, M. E.; Bakac, A.; Espenson, J. H. *J. Am. Chem. Soc.* **1987**, *109*, 4579. (b) Brynildson, M. E.; Bakac, A.; Espenson, J. H. *Inorg. Chem.* **1988**, *27*, 2592. (c) Scott, S. L.; Bakac, A.; Espenson, J. H. *Inorg. Chem.* **1991**, *30*, 4112. (d) Scott, S. L.; Bakac, A.; Espenson, J. H. *J. Am. Chem. Soc.* **1992**, *114*, 4205.
- (2) (a) Kochi, J. K. *Rec. Chem. Prog.* **1966**, *27*, 207. (b) Sheldon, R. A.; Kochi, J. K. *Metal Catalyzed Oxidations of Organic Compounds*; Academic Press: New York, 1981; pp 33-43. (c) Rush, J. D.; Bielski, B. H. *J. Inorg. Chem.* **1985**, *24*, 4282. (d) Kochi, J. K. *Organometallic Mechanisms and Catalysis*; Academic Press: New York, 1978; pp 74-75.
- (3) (a) Hyde, M. R.; Espenson, J. H. *J. Am. Chem. Soc.* **1976**, *98*, 4463. (b) Espenson, J. H.; Martin, A. H. *J. Am. Chem. Soc.* **1977**, *99*, 5953. (c) Heckman, R. A.; Espenson, J. H. *Inorg. Chem.* **1979**, *18*, 38. (d) Bakac, A.; Espenson, J. H. *J. Am. Chem. Soc.* **1986**, *108*, 713. (e) Kim, H. P.; Espenson, J. H.; Bakac, A. *Inorg. Chem.* **1987**, *26*, 4090. (f) Masarwa, M.; Cohen, H.; Meyerstein, D.; Hickman, D. L.; Bakac, A.; Espenson, J. H. *J. Am. Chem. Soc.* **1988**, *110*, 4293. (g) Sadler, N.; Scott, S. L.; Bakac, A.; Espenson, J. H.; Ram, M. S. *Inorg. Chem.* **1989**, *28*, 3951.
- (4) Wang, W.-D.; Bakac, A.; Espenson, J. H. *Inorg. Chem.* **1993**, *32*, 2005.
- (5) Huheey, J. E. *Inorganic Chemistry*; Harper & Row: New York, 1972; pp 160-161.

- (6) *Catalytic Oxidations with Hydrogen Peroxide as Oxidant*; Curci, R., Edwards, E. O., Eds.; Kluwer: Dordrecht, The Netherlands, 1992; Chapter 3.
- (7) Chen, J.-T.; Espenson, J. H. *Inorg. Chem.* **1983**, *22*, 1651.
- (8) Bakac, A.; Orhanovic, M. *Inorg. Chim. Acta* **1977**, *21*, 173.
- (9) (a) Ellis, J. P.; Sykes, A. G. *J. Chem. Soc., Dalton Trans.* **1973**, 2553. (b) Duke, F. R.; Quinney, P. R. *J. Am. Chem. Soc.* **1954**, *76*, 3800.
- (10) (a) Espenson, J. H.; Shaw, K.; Parker, O. J. *J. Am. Chem. Soc.* **1967**, *89*, 5730. (b) Shaw, K.; Espenson, J. H. *Inorg. Chem.* **1968**, *7*, 1619. (c) Shaw, K.; Espenson, J. H. *J. Am. Chem. Soc.* **1968**, *90*, 6622.



were prepared by literature procedures,^{11a} as was $\text{Co}(\text{tim})(\text{H}_2\text{O})_2^{2+}$ ($\text{Co}(\text{tim})^{2+}$).^{11b} The hydroperoxochromium(III) ion, $\text{CrO}_2\text{H}^{2+}$, was prepared by addition of 1 equiv of $\text{Ru}(\text{NH}_3)_6^{2+}$ to a solution of CrO_2^{2+} (0.05–0.3 mM) under Ar. This solution was stored at 0 °C and used within 30 min.

Kinetics. All the kinetic experiments were carried out at 25.0 ± 0.2 °C. Reactions with half-lives of >10 s were conducted by use of a Cary 219 or Shimadzu UV-3101PC spectrophotometer equipped with an internal timer and a thermostated cell-holder. For the reactions with L^1Co^{2+} and Cu^+ , a Durrum stopped-flow instrument was used. Many of the measurements were performed at a constant $[\text{H}^+]$ of 0.10 M. For the reactions carried out at different proton concentrations, the ionic strength was maintained with LiClO_4 . In most of the experiments the kinetics were monitored directly at a wavelength giving the best absorbance change. In the reaction with VO^{2+} the absorbance changes were inconveniently small. This necessitated the use of the kinetic probes ArOH ([2-methyl-2-(3,5-di-*tert*-butyl-4-hydroxyphenyl)propyl]ammo-



nium chloride) or ABTS^{2-} (2,2'-azino-bis(3-ethylbenzothiazoline-6-sulfonate)). The absorbance (D)-time data were fitted to the equation $D_t = D_\infty + (D_0 - D_\infty) \exp(-k_{\text{obs}}t)$ by use of the programs Spectracalc or GraFit.

The activation parameters for the reactions with $\text{CrO}_2\text{H}^{2+}$ and the reactions with H_2O_2 were calculated from the Eyring equation. The kinetic measurements were usually conducted in the temperature range 5.0–40.0 °C.

The stoichiometry of the reaction with Fe^{2+} was determined from the absorbance changes at 240 nm.⁴ For the reaction of $\text{CrO}_2\text{H}^{2+}$ with $\text{Co}(\text{tim})^{2+}$ the measurement was done at 545 nm ($\epsilon = 3450 \text{ M}^{-1} \text{ cm}^{-1}$);¹² $\Delta[\text{Co}(\text{tim})^{2+}]/\Delta[\text{CrO}_2\text{H}^{2+}] = 2.0 \pm 0.1$. For the reactions with L^1Co^{2+} ($\text{L}^1 = [14]\text{aneN}_4$), the measurements were done at 270 nm ($\epsilon = 8300 \text{ M}^{-1} \text{ cm}^{-1}$ for L^1Co^{3+} , $120 \text{ M}^{-1} \text{ cm}^{-1}$ for L^1Co^{2+} , and $1800 \text{ M}^{-1} \text{ cm}^{-1}$ for $\text{CrO}_2\text{H}^{2+}$; $\Delta[\text{L}^1\text{Co}^{2+}]/\Delta[\text{CrO}_2\text{H}^{2+}] = 2.3 \pm 0.1$) and for L^2Co^{2+} ($\text{L}^2 = \text{Me}_6[14]\text{aneN}_4$) at 300 nm ($\epsilon = 5500 \text{ M}^{-1} \text{ cm}^{-1}$ for L^2Co^{3+} , $110 \text{ M}^{-1} \text{ cm}^{-1}$ for L^2Co^{2+} , and $440 \text{ M}^{-1} \text{ cm}^{-1}$ for $\text{CrO}_2\text{H}^{2+}$; $\Delta[\text{L}^2\text{Co}^{2+}]/\Delta[\text{CrO}_2\text{H}^{2+}] = 2.1 \pm 0.1$). The calculations of the molar absorption coefficients at 270 and 300 nm for the cobalt macrocycles utilized concentrations that were determined from the reported spectral data in the visible region.¹³

Results

Self-Decomposition. The decomposition of $\text{CrO}_2\text{H}^{2+}$ is slow ($t_{1/2} \sim 15$ min at room temperature) compared to any of the reactions studied in this work. The products of decomposition in 0.42 M H^+ are Cr^{3+} , H_2O_2 , and O_2 . The presence of H_2O_2 in the decomposed solution was determined kinetically. After a sample of $\text{CrO}_2\text{H}^{2+}$ decomposed, an excess of NaI was added to the solution ($[\text{CrO}_2\text{H}^{2+}]_0 = 0.25 \text{ mM}$, $[\text{I}^-] = 0.014 \text{ M}$, and $[\text{H}^+] = 0.41 \text{ M}$) and the formation of I_3^- monitored spectrophotometrically at 350 nm. The reaction took place with $k = 1.06 \times$

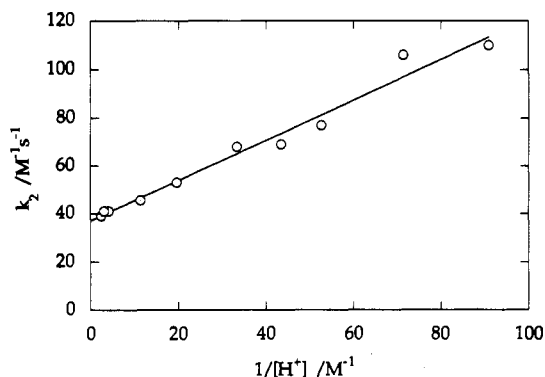


Figure 1. Dependence of k_2 on $[\text{H}^+]$ for the reaction of $\text{CrO}_2\text{H}^{2+}$ with Fe^{2+} at $\mu = 0.41 \text{ M}$ and 25 °C. Each point was calculated from the pseudo-first-order plot which contained at least three different $[\text{Fe}^{2+}]$. The concentrations of Fe^{2+} were in large excess over $[\text{CrO}_2\text{H}^{2+}] = 0.05 \text{ mM}$.

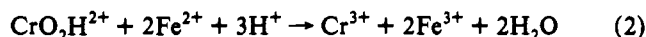
Table I. Kinetic and Stoichiometric Data for the Reaction of $\text{CrO}_2\text{H}^{2+}$ with Fe^{2+} at 25.0 ± 0.2 °C

$[\text{H}^+]$ (M)	$\Delta[\text{Fe}^{2+}]/$ $\Delta[\text{CrO}_2\text{H}^{2+}]$	k_2 ($\text{M}^{-1} \text{ s}^{-1}$)	$[\text{H}^+]$ (M)	$\Delta[\text{Fe}^{2+}]/$ $\Delta[\text{CrO}_2\text{H}^{2+}]$	k_2 ($\text{M}^{-1} \text{ s}^{-1}$)
0.41	2.2	39 ± 1	0.030		68 ± 1
0.32	2.0	41 ± 1	0.023		69 ± 2
0.24	2.3	41 ± 1	0.019		77 ± 2
0.088	2.1	45.6 ± 0.6	0.014		106 ± 6
0.051	2.0	53 ± 2	0.011		110 ± 4

10^{-3} s^{-1} and yielded 0.057 mM I_3^- . Under identical conditions the reaction of I^- with authentic H_2O_2 gave $k = 1.04 \times 10^{-3} \text{ s}^{-1}$. Molecular oxygen was observed in the form of bubbles on the inner surface of the spectrophotometric cell, particularly when the initial concentration of $\text{CrO}_2\text{H}^{2+}$ exceeded 0.1 mM. A quantity of 0.050 mM (1.6 mg/L) oxygen was detected by use of an oxygen sensitive electrode for a solution that initially contained 0.21 mM $\text{CrO}_2\text{H}^{2+}$. The same solution also yielded 0.051 mM H_2O_2 . O_2 does not oxidize I^- rapidly enough under these conditions to interfere with the analysis.

At 0.10 M H^+ , the UV-vis spectra of the decomposed solutions exhibited maxima at 261 and 338 nm, consistent with the presence of HCrO_4^- among the products. The formation of I_3^- by addition of excess I^- (0.0152 M) to this solution took place with an observed-rate constant of $3.35 \times 10^{-3} \text{ s}^{-1}$. Under the same conditions, the observed-rate constants of $2.3 \times 10^{-3} \text{ s}^{-1}$ and $5.22 \times 10^{-4} \text{ s}^{-1}$ were obtained for the reactions of HCrO_4^- and H_2O_2 with I^- , respectively. The kinetic result is qualitatively consistent with both HCrO_4^- and H_2O_2 being present in the decomposed solution. A detailed analysis of the product distribution will be given in the Discussion.

Reactions with Metal Reductants. Iron(II) reduces $\text{CrO}_2\text{H}^{2+}$ according to the stoichiometry of eq 2 with a second order rate



constant of $48 \text{ M}^{-1} \text{ s}^{-1}$.⁴ The stoichiometry is independent of $[\text{H}^+]$ in the range examined, Table I. However, the rate constant increases with a decrease in $[\text{H}^+]$ below 0.1 M. A plot of the second order rate constant against $1/[\text{H}^+]$ is linear, Figure 1. The line drawn corresponds to the equation $k_2/\text{M}^{-1} \text{ s}^{-1} = 37 + 0.84[\text{H}^+]^{-1}$.

Vanadium(II). The reaction of $\text{CrO}_2\text{H}^{2+}$ with V^{2+} was monitored at 270 nm. The $\text{CrO}_2\text{H}^{2+}$ was produced in situ from CrO_2^{2+} and V^{2+} , eq 3. The rate constant for this reaction,^{1b} 2



- (11) (a) Bakac, A.; Espenson, J. H. *J. Am. Chem. Soc.* **1990**, *112*, 2273. (b) Marchaj, A.; Bakac, A.; Espenson, J. H. *Inorg. Chem.* **1993**, *32*, 486. (12) Rillema, D. P.; Endicott, J. F.; Patel, R. C. *J. Am. Chem. Soc.* **1972**, *94*, 394. (13) For $[\text{L}^1\text{Co}(\text{H}_2\text{O})_2]^{3+}$, see: Geiger, T.; Anson, F. C. *J. Am. Chem. Soc.* **1981**, *103*, 7489. For $[\text{L}^2\text{Co}(\text{H}_2\text{O})_2]^{3+}$, see: Roche, T. S.; Endicott, J. F. *Inorg. Chem.* **1974**, *13*, 1575.

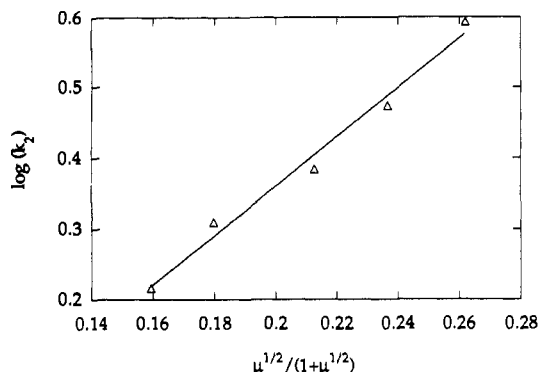


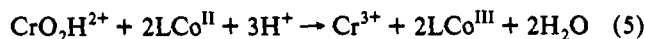
Figure 2. Ionic strength dependence of the second-order rate constant for the reaction of $\text{CrO}_2\text{H}^{2+}$ with V^{2+} at 25 °C. The ionic strength was varied from 0.0165 M to 0.126 M and maintained by perchloric acid only. The slope of the line is 3.5 ± 0.3 .

Table II. Bimolecular Rate Constants for the Reaction of $\text{CrO}_2\text{H}^{2+}$ with Ti^{3+} at $\mu = 0.44$ M and 25 °C

$[\text{H}^+]$ (M)	$[\text{Cl}^-]$ (M)	k_{298} ($\text{M}^{-1} \text{s}^{-1}$)	$[\text{H}^+]$ (M)	$[\text{Cl}^-]$ (M)	k_{298} ($\text{M}^{-1} \text{s}^{-1}$)
0.10	0.44	116 ± 1	0.032	0.028	28 ± 1
0.10	0.25	38 ± 2	0.44	0.028	26.7 ± 0.8
0.10	0.028	28.4 ± 0.8			

$\times 10^5 \text{ M}^{-1} \text{ s}^{-1}$, is sufficiently large to ensure that the formation of $\text{CrO}_2\text{H}^{2+}$ is "instantaneous" on the time scale of the subsequent reaction of interest, eq 4. Reaction 4 obeys mixed second-order kinetics with $k_4 = 3.6 \pm 0.2$, 4.2 ± 0.3 , and $4.5 \pm 0.4 \text{ M}^{-1} \text{ s}^{-1}$ at $\mu = 0.78$ M and $[\text{H}^+] = 0.78$, 0.050, and 0.034 M, respectively. The value of k_4 decreased with decreasing ionic strength. A slope of 3.5 was obtained from the plot of $\log(k_2)$ against $\mu^{1/2}/(1 + \mu^{1/2})$, Figure 2. This is acceptably close to the theoretical value of 4.07, calculated from the Bronsted–Debye–Huckel equation as a product of the ionic charges (4+) and the constant 2A of electroionic theory ($A = 0.509$).

Cobalt(II) Macrocycles. The reactions of $\text{CrO}_2\text{H}^{2+}$ with $\text{L}^1\text{-Co}^{2+}$ and L^2Co^{2+} are accompanied by large absorbance increases in the 300 nm range, corresponding to the formation of Co(III) complexes. Both reactions occur with a 1:2 stoichiometry of eq 5. The reaction with $\text{Co}(\text{tim})^{2+}$ was monitored at 545 nm, and the absorbance change was used to calculate the stoichiometry, which is also given by eq 5.



The kinetic data yielded $k = 1520 \pm 20 \text{ M}^{-1} \text{ s}^{-1}$ for L^1Co^{2+} and 24.8 ± 0.4 for L^2Co^{2+} , independent of $[\text{H}^+]$ in the range 0.020–0.10 M. $\text{Co}(\text{tim})^{2+}$ reacts with $k = 41 \pm 1 \text{ M}^{-1} \text{ s}^{-1}$ at 0.10 M H^+ .

Titanium(III). Stock solutions of Ti^{3+} were prepared by dissolving titanium metal in HCl ,^{8,9} and thus all the kinetic solutions in the $\text{CrO}_2\text{H}^{2+}/\text{Ti}^{3+}$ system necessarily contained some chloride. The reaction was conducted in both chloride and mixed chloride/perchlorate media. In these experiments Ti^{3+} was always added last to avoid the reduction of HClO_4 . (At 0.028 M Cl^- and 0.10 M H^+ , Ti^{3+} reduces ClO_4^- with $k = 0.094 \text{ M}^{-1} \text{ s}^{-1}$ at 40 °C.)^{9b}

The kinetics of the $\text{CrO}_2\text{H}^{2+}/\text{Ti}^{3+}$ reaction were acid and chloride independent at low $[\text{Cl}^-]$ in the acidity range 0.03–0.44 M. At high $[\text{Cl}^-]$ (>0.1 M) the rate constant increased with increasing $[\text{Cl}^-]$, indicating that an additional pathway operates under these conditions. All the data are listed in Table II. Attempts to prepare $\text{CrO}_2\text{H}^{2+}$ by reduction of CrO_2^{2+} by Ti^{3+} were not successful, suggesting an inner-sphere mechanism for this reaction, like that between CrO_2^{2+} and Fe^{2+} .^{1b}

Vanadium(IV). The reaction of $\text{CrO}_2\text{H}^{2+}$ with VO^{2+} takes place with an absorbance change that was too small for direct kinetic measurements in the UV–visible range. The kinetics were thus conducted in the presence of either ABTS^{2-} or ArOH as a

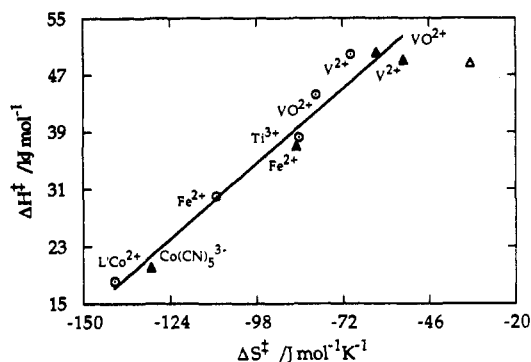
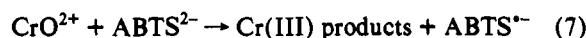
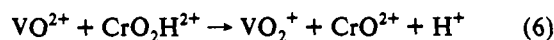


Figure 3. Plot of ΔH^\ddagger vs ΔS^\ddagger for the reactions of transition metal complexes with $\text{CrO}_2\text{H}^{2+}$ (open circles) and with H_2O_2 (solid triangles). The slope defines the isokinetic temperature as 400 K. The open triangle is for the reaction of H_2O_2 with L^2Co^{2+} , which is known to adopt a different mechanism.

kinetic probe. In the presence of ABTS^{2-} as a probe, a two-stage reaction was observed owing to the reaction of ABTS^{2-} with CrO_2^{2+} and the further oxidation of ABTS^{2-} by a reaction product, VO_2^+ :



At sufficiently large concentrations of VO^{2+} (>8 mM) the two stages were separated in time. The standard treatment yielded $k_6 = 8.2 \pm 0.2 \text{ M}^{-1} \text{ s}^{-1}$ for the first stage and $k_8 = 4.0 \pm 0.2 \text{ M}^{-1} \text{ s}^{-1}$ for the second stage, both at $\mu = [\text{H}^+] = 0.50$ M and 25 °C. The reaction of CrO^{2+} with ABTS^{2-} has a rate constant $k_7 = 7.9 \times 10^4 \text{ M}^{-1} \text{ s}^{-1}$ at $[\text{H}^+] = 0.10$ M and 25 °C.^{1d}

The addition of VO^{2+} to a solution containing ArOH and $\text{CrO}_2\text{H}^{2+}$ leads to the formation of ArO^\cdot , as reported earlier.⁴ This phenoxyl radical can be observed by its distinctive UV–vis spectrum in the region 300–450 nm. The kinetic study was done by allowing VO^{2+} (1.8–4.5 mM) to react with $\text{CrO}_2\text{H}^{2+}$ (0.10 mM) in the presence of 2.0 mM ArOH . The absorbance increase at 400 nm, corresponding to the formation of ArO^\cdot , was used to monitor the reaction of VO^{2+} with $\text{CrO}_2\text{H}^{2+}$. The kinetic traces were fitted to a single exponential equation yielding the values of k_ψ . A plot of k_ψ vs $[\text{VO}^{2+}]$ gave a second-order rate constant of $k = 6.0 \pm 0.2 \text{ M}^{-1} \text{ s}^{-1}$ at $\mu = [\text{H}^+] = 0.10$ M and 25 °C. The dependence of the rate constant on $[\text{H}^+]$ was studied at $[\text{CrO}_2\text{H}^{2+}] = 0.035\text{--}0.070$ mM, $[\text{VO}^{2+}] = 0.082\text{--}2.1$ mM, and $[\text{ArOH}] = 1.0$ mM. At $\mu = 0.50$ M and 25 °C the second-order rate constants were 9.5 ± 0.4 and $15.3 \pm 0.3 \text{ M}^{-1} \text{ s}^{-1}$ at $[\text{H}^+] = 0.10$ and 0.030 M. These data and those obtained from the reaction of $\text{CrO}_2\text{H}^{2+}$ with VO^{2+} in the presence of ABTS^{2-} at $[\text{H}^+] = 0.50$ M yield a linear plot of the second-order rate constants against $1/[\text{H}^+]$ with an intercept of $7.5 \text{ M}^{-1} \text{ s}^{-1}$ and a slope of 0.23 s^{-1} .

Copper(I). The reduction of $\text{CrO}_2\text{H}^{2+}$ by Cu^+ takes place with a rate constant $k = 695 \pm 20 \text{ M}^{-1} \text{ s}^{-1}$, independent of $[\text{H}^+]$ in the range 0.010–0.50 M with constant ionic strength of 0.50 M.

Ruthenium(II). The reaction of $\text{CrO}_2\text{H}^{2+}$ with $\text{Ru}(\text{NH}_3)_6^{2+}$ was conducted in 0.10 M $\text{CF}_3\text{SO}_3\text{H}$ to avoid the reaction of $\text{Ru}(\text{NH}_3)_6^{2+}$ with perchlorate.¹⁴ No reaction was observed at $[\text{CrO}_2\text{H}^{2+}] = 0.033$ mM and $[\text{Ru}(\text{NH}_3)_6^{2+}] < 0.8$ mM during the 15-min lifetime of $\text{CrO}_2\text{H}^{2+}$. Thus $k \ll 1 \text{ M}^{-1} \text{ s}^{-1}$ for the reaction of $\text{CrO}_2\text{H}^{2+}$ with $\text{Ru}(\text{NH}_3)_6^{2+}$.

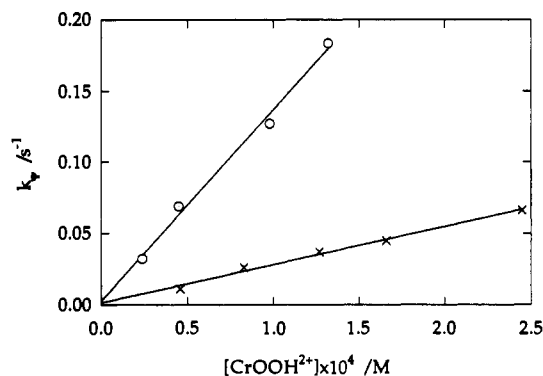
Isokinetic Relationship. The activation parameters for the reactions of $\text{CrO}_2\text{H}^{2+}$ with a number of metal reductants were calculated from their Eyring plots. As shown in Figure 3, ΔH^\ddagger

(14) Kallen, T. W.; Earley, J. E. *Inorg. Chem.* 1971, 10, 1149.

Table III. Summary of the Second-Order Rate Constants and Activation Parameters for the Reactions of $\text{CrO}_2\text{H}^{2+}$ and H_2O_2 with Metal Reductants

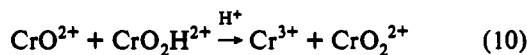
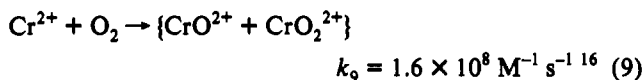
reductants	$\text{CrO}_2\text{H}^{2+}$			H_2O_2		
	k_2 ($\text{M}^{-1} \text{s}^{-1}$)	ΔH^\ddagger (kJ mol^{-1})	ΔS^\ddagger ($\text{J mol}^{-1} \text{K}^{-1}$)	k_2 ($\text{M}^{-1} \text{s}^{-1}$)	ΔH^\ddagger (kJ mol^{-1})	ΔS^\ddagger ($\text{J mol}^{-1} \text{K}^{-1}$)
$\text{Fe}(\text{H}_2\text{O})_6^{2+}$	48.4	29.99 ± 0.68	-110 ± 2	58^a	37.0 ± 1.2^a	-86 ± 4.3^a
$\text{V}(\text{H}_2\text{O})_6^{2+}$	2.5	49.93 ± 0.84	-69.9 ± 2.8	17^b	49.1 ± 3.0	-53.8 ± 10.2
$\text{Ti}(\text{H}_2\text{O})_6^{3+}$	28	38.21 ± 0.83	-85.3 ± 2.8	920^c		
VO^{2+}	6	44.2 ± 2.0	-80.2 ± 6.9	5.8^c	50.2 ± 2.1	-62 ± 7
L^1Co^{2+}	1530			3970^d		
L^2Co^{2+}	24	18.17 ± 1.26	-140.5 ± 4.4	265^d		
$\text{Co}(\text{tim})^{2+}$	41			142^d		
Cu^+	700			4100^e		
$\text{Ru}(\text{NH}_3)_6^{2+}$	NR			$<10^{-2}^f$		

^a Reference 15a. ^b Reference 3c. ^c Calculated from ref 20. ^d Reference 2c. ^e Reference 2f. ^f Pladzewicz, J. R.; Meyer, T. J.; Broomhead, J. A.; Taube, H. *Inorg. Chem.* 1973, 12, 639.

**Figure 4.** Dependence of the observed rate constants on the concentration of $\text{CrO}_2\text{H}^{2+}$ in H_2O (open circles) and in D_2O (crosses) for the reaction of $\text{CrO}_2\text{H}^{2+}$ with CrO^{2+} in 0.10 M $\text{H}(\text{D})\text{ClO}_4$ at 25 °C.

is a linear function of ΔS^\ddagger not only for $\text{CrO}_2\text{H}^{2+}$ but for H_2O_2 as well. The slope of the line yields the isokinetic temperature of $400 \pm 30 \text{ K}$ or $130 \pm 10 \text{ °C}$. The activation parameters for the reactions of H_2O_2 and $\text{CrO}_2\text{H}^{2+}$ are given in Table III, and the data for the reactions of H_2O_2 with $\text{Co}(\text{CN})_5^{3-}$ and with Fe^{2+} were obtained from the literature.¹⁵

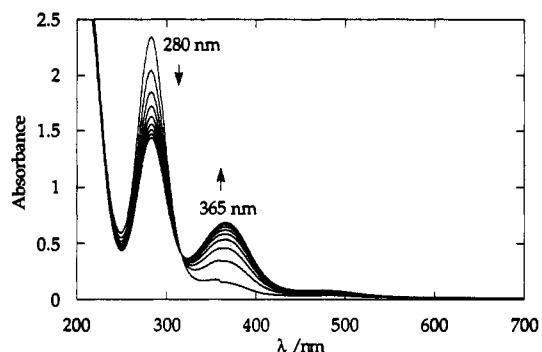
Oxidation of $\text{CrO}_2\text{H}^{2+}$. Addition of Cr^{2+} (0.2 mM) to an air-saturated solution of methanol-free $\text{CrO}_2\text{H}^{2+}$ (0.05 mM) caused the absorbance in the UV to increase. The spectrum of the product matches exactly that of CrO_2^{2+} . The chemistry involved is shown in eqs 9 and 10.



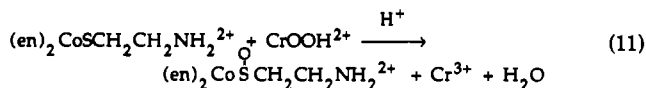
With $\text{CrO}_2\text{H}^{2+}$ present in a large excess over CrO^{2+} , the formation of CrO_2^{2+} follows first-order kinetics. The observed rate constants vary linearly with the concentration of $\text{CrO}_2\text{H}^{2+}$ and yield $k_{10} = (1.34 \pm 0.06) \times 10^3 \text{ M}^{-1} \text{ s}^{-1}$ at 25 °C and 0.10 M H^+ . When all of the solutions (Cr^{2+} , DClO_4 , $\text{Ru}(\text{NH}_3)_6^{2+}$, $\text{CrO}_2\text{D}^{2+}$) were prepared in D_2O , the rate constant was significantly smaller, $266 \pm 10 \text{ M}^{-1} \text{ s}^{-1}$, giving $k_{\text{H}}/k_{\text{D}} = 5.0$, as shown in Figure 4.

There was no reaction between $\text{CrO}_2\text{H}^{2+}$ (0.15 mM) and HCrO_4^- (0.03–0.08 mM) in 10 min at 0.1 M H^+ .

- (15) (a) For the reaction of Fe^{2+} with H_2O_2 , values were calculated from the data in: Hardwick, T. J. *Can. J. Chem.* 1957, 35, 428. Barb, W. G.; Baxendale, J. H.; George, P.; Hargrave, K. R. *Trans. Faraday Soc.* 1951, 47, 462. (b) For the reaction of $\text{Co}(\text{CN})_5^{3-}$ with H_2O_2 , see: Chock, P. B.; Dewar, R. B. K.; Halpern, J.; Wong, L.-Y. *J. Am. Chem. Soc.* 1969, 91, 82.
- (16) (a) Ilan, Y. A.; Czapaki, G.; Ardon, M. *Isr. J. Chem.* 1975, 13, 15. (b) Sellers, R. M.; Simic, M. G. *J. Am. Chem. Soc.* 1976, 98, 6145.

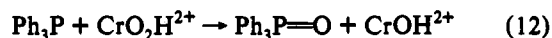
**Figure 5.** Repetitive scan spectra (every 100 s) for the reaction of 0.16 mM $\text{CrO}_2\text{H}^{2+}$ with 0.19 mM $[(\text{en})_2\text{Co}(\text{SCH}_2\text{CH}_2\text{NH}_2)]^{2+}$, showing the disappearance of $[(\text{en})_2\text{Co}(\text{SCH}_2\text{CH}_2\text{NH}_2)]^{2+}$ at 280 nm and the growth of the product at 365 nm.

Reactions with Nucleophiles. $(\text{en})_2\text{CoSCH}_2\text{CH}_2\text{NH}_2^{2+}$ reacts with $\text{CrO}_2\text{H}^{2+}$ according to eq 11. The rate constant $k_{11} = 20.5$



$\pm 0.4 \text{ M}^{-1} \text{ s}^{-1}$ at 0.10 M H^+ was obtained from a plot of k_{obs} vs $[(\text{en})_2\text{CoSCH}_2\text{CH}_2\text{NH}_2^{2+}]$. The formation of $(\text{en})_2\text{CoS}(\text{O})\text{CH}_2\text{CH}_2\text{NH}_2^{2+}$, an oxygen transfer product, is clearly indicated by the growing absorption maximum at 365 nm.¹⁷ The reaction is clean with an isosbestic point at 310 nm as shown in the repetitive-scan spectra in Figure 5.

Triphenylphosphine. Because of the low solubility of Ph_3P in H_2O , the reaction of PPh_3 with hydroperoxides was studied in 1:1 $\text{CH}_3\text{CN}/\text{H}_2\text{O}$ (v/v) at 0.10 M H^+ . Under these conditions the reaction of H_2O_2 with PPh_3 took place with a 1:1 stoichiometry and a rate constant $2.94 \pm 0.08 \text{ M}^{-1} \text{ s}^{-1}$. The reaction with $\text{CrO}_2\text{H}^{2+}$ gave $k = 75 \pm 3 \text{ M}^{-1} \text{ s}^{-1}$.



Bromide Ions. The absorbance increase at 260 nm, corresponding to the formation of Br_3^- , was used to follow the reaction of $\text{CrO}_2\text{H}^{2+}$ with Br^- . To obtain sufficient absorbance change, $>30 \text{ mM}$ Br^- was used to react with $\text{CrO}_2\text{H}^{2+}$ (0.05–0.1 mM). The acid dependence was studied in the range 0.10–0.75 M H^+ at 2.0 M ionic strength. The second-order rate constants are 0.063, 0.19, 0.31, and 0.41 $\text{M}^{-1} \text{ s}^{-1}$ at 0.10, 0.25, 0.50, and 0.75 M H^+ , respectively. A plot of the second-order rate constants against $[\text{H}^+]$ yields a straight line described by the equation $k_2/\text{M}^{-1} \text{ s}^{-1} = 0.035 + 0.52[\text{H}^+]$. The oxidation of bromide by H_2O_2 takes

- (17) (a) Adzami, I. K.; Deutsch, E. *Inorg. Chem.* 1980, 19, 1366. (b) Adzami, I. K.; Libson, K.; Lydon, J. D.; Elder, R. C. Deutsch, E. *Inorg. Chem.* 1979, 18, 303.

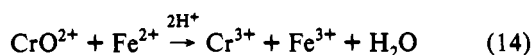
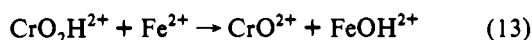
place according to the same general rate law with $k = 3.8 \times 10^{-7} + 2.3 \times 10^{-4}[\text{H}^+]$.¹⁸

Discussion

Mechanism. The reduction of H_2O_2 and ROOH by transition metal complexes requires precoordination of peroxide to the metal. The reaction rate is therefore governed not only by the driving force for these reactions but also by the ligand substitution rates of the metal complexes. For example, V^{2+} reduces H_2O_2 more slowly than Fe^{2+} does ($k_v = 17 \text{ M}^{-1} \text{ s}^{-1}$, compared to $k_{\text{Fe}} = 58 \text{ M}^{-1} \text{ s}^{-1}$), even though the reduction potential of $\text{V}^{3+}/\text{V}^{2+}$ ($E^\circ = -0.255 \text{ V}$) is over 1 V more negative than that of $\text{Fe}^{3+}/\text{Fe}^{2+}$ ($E^\circ = 0.77 \text{ V}$). The same reactivity order is found in the reactions of $\text{CrO}_2\text{H}^{2+}$ with transition metal reductants, Table III.

The most striking feature of the data in Table III is the similarity of rate constants for the reactions of H_2O_2 and $\text{CrO}_2\text{H}^{2+}$ with common reductants. As a rule, the reactions of $\text{CrO}_2\text{H}^{2+}$ are slower, but the difference is small. The most obvious interpretation is that the two peroxides react by the same mechanism and that the replacement of one H^+ by Cr^{3+} has little influence on the reduction potential of H_2O_2 .

With the possible exception of Cu^+ ,^{2f} the aqueous reactions of H_2O_2 with transition metal complexes in Table III are believed^{2,3} to proceed by a one-electron, Fenton-type mechanism, eq 1b. As for the reactions of $\text{CrO}_2\text{H}^{2+}$, the trapping experiments with ArOH and oxalate reported previously strongly support the intermediacy of CrO^{2+} in the reaction with Fe^{2+} .⁴ Similarly, the formation of ArO \cdot in the reaction of $\text{CrO}_2\text{H}^{2+}$ with VO^{2+} in the presence of ArOH provides evidence for the intermediacy of CrO^{2+} in this system as well. The observed reactivity order for the series of reductants and the isokinetic relationship in Figure 3 suggest that the rest of the reactions in Table III also take place by a modified Fenton mechanism, shown for Fe^{2+} in eqs 13 and 14.



The reaction of L^2Co^{2+} with H_2O_2 has a 1:1 stoichiometry, whereas the corresponding reaction with $\text{CrO}_2\text{H}^{2+}$ has $\Delta[\text{CrO}_2\text{H}^{2+}]/\Delta[\text{L}^2\text{Co}^{2+}] = 0.50$. It was proposed previously^{2c} that the H_2O_2 reaction starts out with a Fenton-type step, but the product OH \cdot is captured by the macrocyclic ligand, possibly in a single step. The chromyl ion, on the other hand, is much less reactive toward C-H bonds^{1d} and is therefore released into solution.

Let us assume that the much lower reactivity of CrO^{2+} , relative to HO \cdot , in redox reactions and hydrogen atom abstractions is thermodynamic in origin. If this is true, then the similarity of the kinetic data for H_2O_2 and $\text{CrO}_2\text{H}^{2+}$ has an interesting implication: the substitution of H^+ by Cr^{3+} lowers the free energy content of H_2O_2 and HO \cdot by an approximately equal amount. Thus despite the larger absolute reduction potentials of the hydrogen species relative to the chromium-substituted ones, the free energy change in reactions 1a and 1b is approximately the same. Additional data are required to test this proposal.

Effect of H^+ . The kinetics of the reaction of Fe^{2+} with H_2O_2 is acid independent at $[\text{H}^+] > 0.01 \text{ M}$.^{15a} Below this concentration the rate constant increases with decreasing acidity, probably because of the pH dependence of the $\text{Fe}^{\text{III}}/\text{Fe}^{\text{II}}$ reduction potential.¹⁹ Similar observations were made in the reactions of H_2O_2 with Ti^{3+} and VO^{2+} at 0.003–1 M HClO_4 .²⁰

The rate law for the reaction of $\text{CrO}_2\text{H}^{2+}$ with Fe^{2+} has a major acid independent term ($k = 37 \text{ M}^{-1} \text{ s}^{-1}$) and a term inversely

Table IV. Comparison of the Kinetic Data for the Reactions of Nucleophiles with $\text{CrO}_2\text{H}^{2+}$ and with H_2O_2 (25 °C, 0.10 M H^+)

reagent	$k_{298} (\text{M}^{-1} \text{ s}^{-1})$		
	PPh_3	Br^-	CoSR^{2+}
$\text{CrO}_2\text{H}^{2+}$	75	0.063	20.5
H_2O_2	3	0.000 23 ^a	1.36 ^b

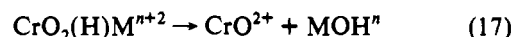
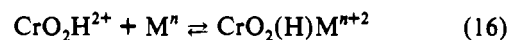
^a Reference 18. ^b Reference 17a.

proportional to $[\text{H}^+]$ in the range 0.011–0.41 M, eq 15. All the other reactions in Table III are acid independent, except the reaction with VO^{2+} .

$$k_{\text{Fe}} = k_0 + k[\text{H}^+]^{-1} \quad (15)$$

The precise value of the $\text{p}K_a$ of $\text{Cr}(\text{H}_2\text{O}_2)^{3+}$ is not known, although one can reasonably place it in the range 1–3.^{1c} Both forms, $\text{Cr}(\text{H}_2\text{O}_2)^{3+}$ and $\text{CrO}_2\text{H}^{2+}$, might therefore be present under our experimental conditions. The pH independence of most of the reactions in Table III indicates that the reactivities of the two forms are similar or that the $\text{p}K_a$ lies outside the estimated limit.

The detailed mechanism for the reduction of $\text{CrO}_2\text{H}^{2+}$ by transition metal complexes is shown in eqs 16 and 17. The



formation and dissociation of the binuclear peroxo intermediate, reaction 16, may or may not be acid dependent. Note that in the reductions of H_2O_2 by low-valent transition metal complexes there is typically no acid dependence associated with this step. VO^{2+} is a notable exception.²⁰ However, the substitution of $\text{CrO}_2\text{H}^{2+}$ for H_2O_2 causes an increase in the charge on the peroxo intermediate by two units, which will certainly cause a dramatic change in its $\text{p}K_a$. Thus the reverse reaction, eq 16, and the electron-transfer/product forming step, eq 17, may be acid catalyzed. As long as the kinetic order in H^+ is the same for reactions 16 and 17, the overall kinetics will be acid independent, eq 18, as observed experimentally. The $1/[\text{H}^+]$ term in the iron(II) case may indicate that FeOH^+ is much more reactive than Fe^{2+} .

$$k_{\text{obs}} = k_{16}k_{17}/(k_{-16} + k_{17}) \quad (18)$$

Oxygen Transfer Reactions. As shown in Table IV, the reactions of $\text{CrO}_2\text{H}^{2+}$ with nucleophiles are about 20 times faster than the corresponding reactions with H_2O_2 . Oxidations of coordinated^{17a} and free thiols²¹ by H_2O_2 take place by nucleophilic attack at the O–O bond^{17a,21} with the kinetics described by eq 19.

$$\text{rate} = (k_1 + k_2[\text{H}^+])[\text{H}_2\text{O}_2][\text{Nuc}] \quad (19)$$

It has been shown^{17a} that the energetics of the O–O bond cleavage control the oxidation of coordinated thiols. For the reaction of $\text{CrO}_2\text{H}^{2+}$ with the (thiolato)cobalt complex, the addition of ArOH has no effect on the kinetics or on the yield of the (sulfenato)-cobalt product. Also no ArO \cdot was observed in this reaction, which indicates that CrO^{2+} was not produced. We believe that the oxidation of $(\text{en})_2\text{CoSCH}_2\text{CH}_2\text{NH}_2^{2+}$ by $\text{CrO}_2\text{H}^{2+}$ proceeds by the same mechanism as the H_2O_2 reaction. The weaker O–O bond and the positive charge on $\text{CrO}_2\text{H}^{2+}$ may be the reason for the 20-fold acceleration compared to the hydrogen peroxide reaction. Unlike H_2O_2 , $\text{CrO}_2\text{H}^{2+}$ does not oxidize $(\text{en})_2\text{CoS}(\text{O})\text{CH}_2\text{CH}_2\text{NH}_2^{2+}$ to the sulfinato complex $(\text{en})_2\text{CoS}(\text{O})_2\text{CH}_2\text{CH}_2\text{NH}_2^{2+}$ at appreciable rates.

(18) Mohammad, A.; Liebhaufsky, H. A. *J. Am. Chem. Soc.* 1934, 56, 1680.

(19) Wells, C. F.; Salam, M. A. *J. Chem. Soc. A*, 1968, 24.

(20) Samuni, A.; Meisel, D.; Czapski, G. *J. Chem. Soc., Dalton Trans.* 1972, 1273.

(21) Hoffmann, M.; Edward, J. O. *Inorg. Chem.* 1977, 16, 3333.

The oxidation of tertiary phosphines by H_2O_2 has been used to synthesize tertiary phosphine oxides,²² but no detailed kinetic studies have been carried out. To compare the reactivities of H_2O_2 and $\text{CrO}_2\text{H}^{2+}$, the reactions of both hydroperoxides with PPh_3 were studied kinetically in 1:1 $\text{CH}_3\text{CN}/\text{H}_2\text{O}$. Similar to the case for other nucleophiles in Table IV, the reaction of H_2O_2 with PPh_3 is about 20 times slower than the corresponding $\text{CrO}_2\text{H}^{2+}$ reaction.

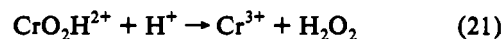
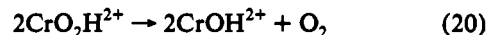
The oxidation of halides by H_2O_2 has been known to follow the same kinetic expression as shown in eq 19.¹⁸ The acid-dependent kinetics found in the reaction of Br^- with $\text{CrO}_2\text{H}^{2+}$ resemble those observed in the corresponding H_2O_2 reaction, suggesting the same mechanism for the two peroxides.

Oxidation of $\text{CrO}_2\text{H}^{2+}$. Hydrogen peroxide and alkyl hydroperoxides can be oxidized by strong oxidizing agents, such as Ce^{IV} and Mn^{III} .²³ Oxidation of $\text{CrO}_2\text{H}^{2+}$ by Ce^{IV} to produce CrO_2^{2+} has been used initially to characterize $\text{CrO}_2\text{H}^{2+}$ as an intact product of the one-electron reduction of CrO_2^{2+} .^{1c,4} In this work we studied the oxidation of $\text{CrO}_2\text{H}^{2+}$ by CrO^{2+} , eq 10. The experimentally observed stoichiometry of eq 10 and the kinetic isotope effect $k_{\text{H}}/k_{\text{D}} = 5.0$ are consistent with hydrogen atom abstraction by CrO^{2+} . However, the isotope effect is a combination of contributions from solvent and coordinated water in addition to that from the hydroperoxo group, which makes the mechanistic assignment less than definitive.

The two peroxides, H_2O_2 and $\text{CrO}_2\text{H}^{2+}$, have similar reactivities toward both oxidants and reductants examined in this work. The $\text{CrO}_2\text{H}^{2+}$ is a somewhat better reductant and H_2O_2 a better oxidant, but differences are generally small and can probably be rationalized by charge effects and minor differences in the redox potentials and O—O bond strengths.

Decomposition of $\text{CrO}_2\text{H}^{2+}$. At 0.4 M H^+ and <0.1 mM $\text{CrO}_2\text{H}^{2+}$, the hydroperoxochromium ion has a half-life of ca. 15

min at 25 °C. Our preliminary work indicates that the decomposition becomes faster at higher initial concentrations, indicating a greater than first-order dependence on $\text{CrO}_2\text{H}^{2+}$. This kinetic behavior and the formation of O_2 as one of the decomposition products indicate that the coordinated peroxide may be decomposing by disproportionation (eq 20), similar to



the parent H_2O_2 . The effect of H^+ on the kinetics and the increased yields of H_2O_2 at higher H^+ are consistent with acidolysis of eq 21 being also a major pathway. This type of decomposition has been observed in other metal hydroperoxide systems as well.²⁴ At 0.10 M H^+ , the UV-vis spectra of the decomposed solutions and the kinetic result are consistent with both HCrO_4^- and H_2O_2 being present in the decomposed solution. Equation 22 is proposed to account for this decomposition route, which is also a disproportionation reaction; however, this time it occurs between Cr(III) and coordinated peroxide. At high concentration of H^+ , eq 21 is dominant but eq 22 becomes a major path when the concentration of H^+ is low. The kinetic traces for the decomposition of $\text{CrO}_2\text{H}^{2+}$ were complicated by the generation of gas bubbles, which precluded the detailed analysis of the three processes.

Acknowledgment. This work was supported by the grant from the National Science Foundation (CHE-9007283). Some of the experiments were conducted with the use of the facilities of the Ames Laboratory.

(22) Ketelaere, D.; Kelen, V.; Eeckhaut, Z. *Phosphorus* 1974, 5, 43.

(23) Kochi, J. K. *Organometallic Mechanisms and Catalysis*; Academic Press: New York, 1978; pp 60–80.

(24) (a) Gubelmann, M. H.; Ruttimann, S.; Bocquet, B.; Williams, A. F. *Helv. Chim. Acta* 1990, 73, 219. (b) Michelin, R. A.; Ros, R.; Strukul, G. *Inorg. Chim. Acta* 1979, 37, L491. (c) Roberts, H. L.; Symes, W. R. *J. Chem. Soc. A* 1968, 1450. (d) Muto, S. *Chem. Lett.* 1975, 809.